Proceedings of the XII Serbian-Bulgarian Astronomical Conference (XII SBAC) Sokobanja, Serbia, September 25-29, 2020
Editors: L. Č. Popović, V. A. Srećković, M. S. Dimitrijević and A. Kovačević
Publ. Astron. Soc. "Rudjer Bošković" No 20, 2020, 51-59

ANALYSIS OF THE DENSITY DISTRIBUTION IN STAR-FORMING CLOUDS: EXTRACTION OF A SECOND POWER-LAW TAIL

LYUBOV MARINKOVA[1], TODOR V. VELTCHEV[1] and SAVA DONKOV[2]

[1]*Department of Astronomy, University of Sofia, James Bourchier Blvd. 5, Sofia 1164, Bulgaria*
[2]*Department of Applied Physics, Faculty of Applied Mathematics, Technical University of Sofia, 8 Kliment Ohridski Blvd., BG-1000, Sofia, Bulgaria*
E-mail: ln@phys.uni-sofia.bg, eirene@phys.uni-sofia.bg, savadd@tu-sofia.bg

Abstract. Clues to understand physics and evolution of molecular clouds can be provided through analysis of the probability density functions of mass density (ρ-pdf) and of column density (N-pdf). Many numerical simulations show that a power-law tail (PLT) emerges at the high-density end of the ρ-pdf at advanced evolutionary stages of star-forming clouds. Later, at the stage of collapse of first formed protostellar cores, a second, shallower PLT appears (Kritsuk et al. 2011). Double PLTs have been also detected in N-pdfs from *Herschel* maps in several star-forming regions (Schneider et al. 2015, 2020).

However, it is difficult to estimate the parameters of the second PLT due to resolution constraints. We propose a technique for extraction of a second PLT in ρ/N-pdfs which is an extension of the method of Veltchev et al. (2019) for extraction of single PLTs from arbitrary density distributions. The technique is applied to a set of hydrodynamical simulations of isothermal self-gravitating clouds. The results confirm the emergence of a shallower second PLT in ρ-pdfs at timescales, comparable with the free-fall time of the average density in the box. Second PLTs are detected also in N-pdfs derived from *Herschel* maps of a low-mass (Pipe) and high-mass (M 17) star-forming regions.

1. INTRODUCTION

Stars are born in molecular clouds (MCs), therefore the study of star formation requires understanding of the morphological and kinematical evolution of MCs. Initial stage of cloud formation is the compression of interstellar warm atomic gas by supersonic flows followed by rapid cool down due to non-linear thermal instabilities (see Ballesteros-Paredes et al. 2020, for a review). Stars begin to form when self-gravity in the cloud takes slowly over and local sites of gravitational collapse emerge. This evolution could be described in terms of detection and

physical parameters of substructures (clumps, cores) or in terms of indicators of general structure.

An important indicator of general cloud structure is the probability distribution function (pdf) of mass density (ρ-pdf) and its analysis can give clues to understand the physics and evolution of the cloud. From observations, one could derive the pdf of column density (N-pdf), which turns out to be morphologically analogous to the ρ-pdf. In isothermal, non-gravitating fluids with well developed supersonic turbulence the ρ-pdf is mostly lognormal (e.g. Vázquez-Semadeni 1994, Li, Klessen and Mac Low 2003, Federrath et al. 2010), i.e. can be fitted by lognormal function of type:

$$p(s)\,ds = \frac{1}{\sqrt{2\pi\sigma^2}} \exp\left[-\frac{1}{2}\left(\frac{s-s_{\max}}{\sigma}\right)^2\right] ds\,,$$

where s=log(ρ/ρ_0) and $s_{\max}$ are the logdensity (with normalization to the mean density ρ_0) and its value at the distribution peak and σ is the standard deviation. This result was confirmed by numerous simulations. At advanced evolutionary stages, when self-gravity becomes important in the energy balance in the cloud, a power-law tail (PLT) with functional form

$$p(s) = A\exp(qs) = A(\rho/\rho_0)^q \;, \quad s \geq s_{\rm PLT}\,,$$

emerges at the high-density end of the pdf, where A is a constant, q is the power index and the deviation point (DP) $s_{\rm PLT}$ from lognormality separates the two regimes (Klessen 2000, Kritsuk, Norman and Wagner 2011, Federrath and Klessen 2013). The evolution of the N-pdf turns out to be morphologically similar (see, e.g, Ballesteros-Paredes et al. 2011, Koertgen, Federrath and Banerjee 2019). Example of a pdf with main lognormal part and a PLT is shown in Fig. 1.

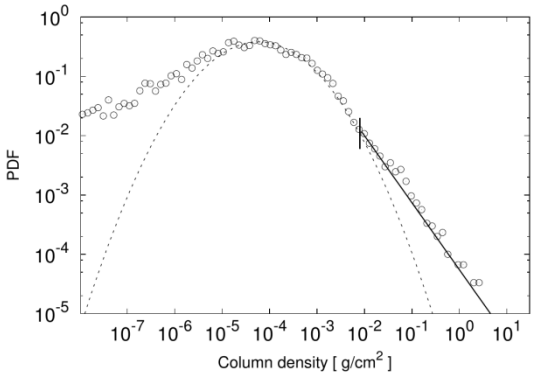

Figure 1: N-pdf derived from a run of the SILCC (SImulating the LifeCycle of molecular Clouds) simulations (Girichidis et al. 2018).

In the course of further MC evolution the main part of the ρ-pdf retains its (quasi-) lognormal shape. On the other hand, the slope of the PLT gets slowly shallower, tending toward a constant value while DP shifts to lower values.

Some numerical studies with high resolution (reaching down AU scales) hint at emergence of a *second* PLT at advanced evolutionary stages of star-forming clouds. For instance, Kritsuk et al. (2011) found that the density distribution in self-gravitating clouds develops an extended PLT with a slope of about −1.7 at high densities on top of the usual lognormal. The tail departs from the initial lognormal distribution already at $\rho/\rho_0 \sim 10$ and continues straight for nearly 10 dex in $p(s)$ and more than 6 dex in density. As the simulation progresses, the slope continues to evolve slowly toward shallower values reaching q=−1.67 at the end of the simulation. An even shallower tail is detected at densities $\rho/\rho_0 \geq 10^7$. This might indicate mass pile-up due to an additional support against gravity due to conservation of angular momentum (rotation of prestellar cores), strong magnetic fields in the densest parts of MC, change in the equation of state (non-isothermality; see Donkov et al. in this issue) or all these factors.

2. EXTRACTION OF POWER-LAW TAILS OF THE PDF

There is a methodological problem with the extraction of the PLT: its characteristics and those of the lognormal fitting function are obviously interdependent. Let us review the usual procedure to extract the PLT: (i) Find the best lognormal fit of the main pdf part (e.g. using the χ^2 goodness); (ii) Estimate the DP of the distribution from the lognormal fit (e.g. using the 3σ criterion, where σ is the Poissonian data uncertainty in the considered bin). (iii) Fit the rest of the distribution with a PL function. Such an approach rests on the assumption that the main pdf part is lognormal and thus the resulting DP and the PL slope depend on the parameters of the lognormal fit. However, if the PL regime is to be interpreted as a signature of the impact of self-gravity, then the slope value is an indicator of the cloud's evolutionary stage. We need a method to extract the PLT on minimal assumptions about the rest of the density distribution.

Such approach was recently proposed by Veltchev et al. (2019; hereafter V19) and named adapted BPLFIT method. The power-law fit of a distribution (or part of it) is derived by use of Kolmogorov-Smirnov (KS) goodness-of-fit statistics. The procedure does not rule out that other, non-power-law, functions might better fit the observed distribution – it simply derives the range and the slope of the best possible power-law fit. This method can deal with large datasets of size $< 10^5$ points from numerical simulations and high-resolution imaging of MCs and is applicable to linear, logarithmic and arbitrary binning schemes. Average slope and DP are derived as the number of bins is varied and are not sensitive to spikes and other local features of the distribution's tail.

3. TECHNIQUE FOR EXTRACTION OF A SECOND POWER-LAW TAIL

The adapted BPLFIT method can be elaborated further for detection of a second PLT (if present). The PLFIT procedure searches for the PLT of the considered PDF by use of the KS statistic for given lower cutoff $x_{\min}$:

$$D = \max_{x_i \geq x_{\min}} |S(x_i) - P(x_i)|$$

where $S(x_i)$ is the cumulative distribution function (CDF) of the data and $P(x)$ is the CDF of the best-fitting power-law model in the range $x_i \geq x_{\min}$. The value of $x_i \geq x_{\min}$ which minimizes D and the corresponding power-law index are selected as DP and slope of the PLT, respectively. If no lower cutoff is introduced, $x_{\min}$ is simply the lower limit of the data set (in our case, the minimal logdensity) – V19 extracted PLTs from numerical and observational PDFs in this way. Gradual increase of $x_{\min}$ constrains the considered data set and, hence, the set of values $|S(x_i) - P(x_i)|$ to obtain the KS statistic. In particular, such approach may help to detect a second PLT corresponding to higher logdensities, for some $x_{\min}$ which exceeds the DP of the single (first) PLT.

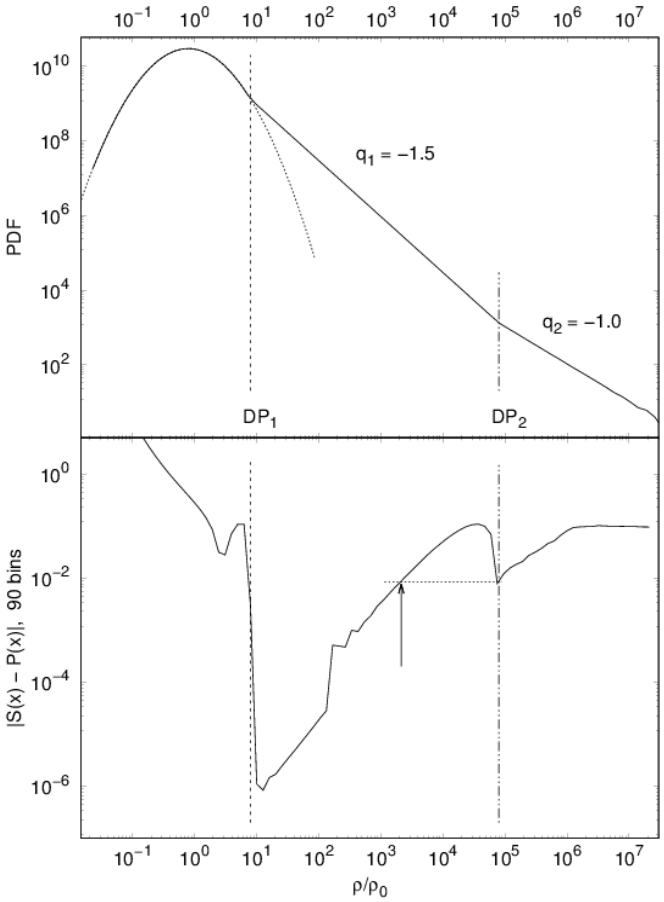

Figure 2: Illustration of the suggested method for extraction of two PLTs as applied to an analytic binned PDF (top panel; solid) with main part fitted by lognormal function (dotted) and two PLTs.
Bottom panel displays the function $|S(x) - P(x)|$ (see text).

To illustrate this we construct an analytic PDF (Fig. 2, top) whose shape and parameters resemble the one obtained in the numerical study of Kritsuk et al. (2011). The main part is lognormal while the high-density one consists of two PLTs with deviation points DP_1 and DP_2 and slopes $q_1 = -1.5$ (typical for evolved self-gravitating clouds, Girichidis et al. 2014) and $q_2 = -1$.

An example of the function $|S(x) - P(x)|$ for a large total number of bins (i.e. small bin size) is shown in Fig. 2, bottom. As expected, the value of $|S(x) - P(x)|$ is large in the range $x < DP_1$ which defines the lognormal part of the PDF. The deviation points of the two PLTs correspond to pronounced local minima, with a local maximum located in between. As long as $x_{min} < DP_1$, the adapted BPLFIT will extract a single PLT with $DP = DP_1$ and slope q_1 (Fig. 3). Choices of lower cutoffs x_{min} □ DP_1 still yield a single PLT with gradually changing parameters. The second PLT with $DP = DP_2$ will be detected at a cutoff with $|S(x_{min})-P(x_{min})|$ □ $|S(DP_2) - P(DP_2)|$ (arrow and dotted line in Fig. 2, bottom) – then the procedure selects $x_i = DP_2$ (cf. Fig. 3) since with this choice the local maximum at $\rho/\rho_0 \approx 4 \times 10^4$ is excluded.

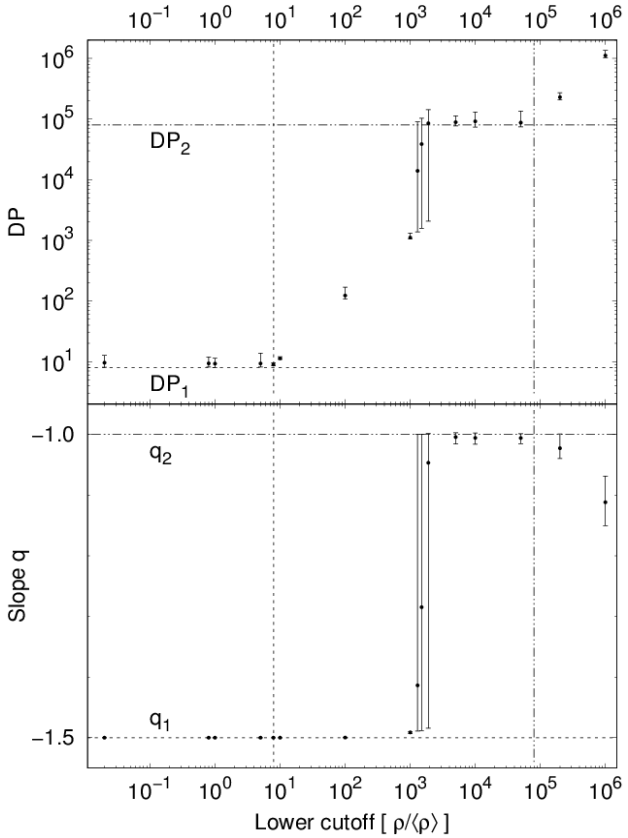

Figure 3: Dependence of the extracted PLT parameters on the chosen lower cutoff of the tested PDF (cf. Fig. 2).

In the next two Sections we present tests of the suggested method to numerical and observational data.

4. RESULTS FROM NUMERICAL DATA: DENSITY PDF

We use data from a set of 6 hydrodynamical simulations of self-gravitating clouds called HRIGT (High-Resolution Isothermal Gravo-Turbulent). The size of the numerical box is 0.5 pc, about the scale of typical large clumps in MCs. The complexity in physical modeling is reduced in favor of higher resolution and significantly higher adaptive refinement (from 256^3 up to 32768^3 cells) – thus the resolution can reach ~3 AU in high-density zones. The gas is isothermal (T=10 K) and uniformly distributed at the initial point in time. The total mass in the box is chosen to be 85 and 426 $M_\odot$ in the different runs which corresponds to 32 and 354 Jeans masses ($M_{J,0}$). The initial turbulent velocities are constructed in Fourier space with a peak of the power spectrum at k = 2, i.e. half of the box size. We distinguish between purely compressive, purely solenoidal and naturally mixed velocities (Federrath, Klessen and Schmidt 2008).

The chosen HRIGT runs differ in total mass, realizations of velocity field, turbulent driving and duration in units of free-fall time t_{ff}. In general, the runs with total mass of 354 $M_{J,0}$ have been stopped at earlier points in time (<1.5 t_{ff}). Therefore one would expect that in those cases the extracted PLTs in the mass-density pdf will be steeper. Fig. 4 demonstrates that this is indeed the case in regard to the *first* PLT. The obtained slopes are in a good agreement with the theoretical limit q~−1.5 for evolved self-gravitating clouds substantiated by Girichidis et al. (2014).

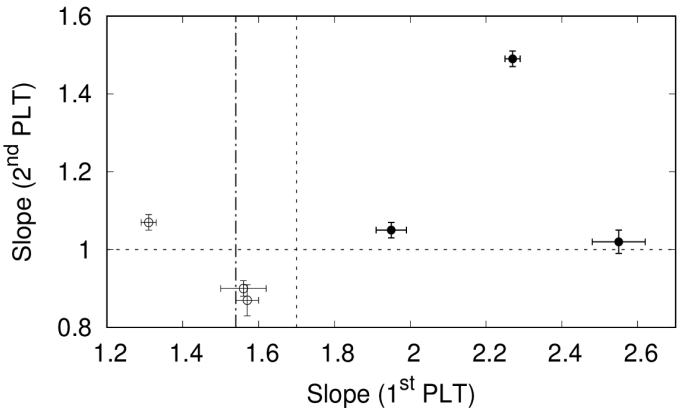

Figure 4: Comparison between the slopes of the extracted first and second PLT from the HRIGT simulations: with 32 (open circles) and 354 (filled circles) Jeans masses. The corresponding final values from Kritsuk et al. (2011; dashed) and the limiting value from Girichidis et al. (2014; dash-dotted) are plotted.

In regard to the *second* PLT, all HRIGT runs yield similar results, independent on the total mass in the box. The slopes are around -1 (and even shallower) which confirms the result of Kritsuk et al. (2011).

5. RESULTS FROM OBSERVATIONAL DATA: COLUMN-DENSITY PDF

We test the method also to *N*-pdfs from *Herschel* observations of several star-forming regions. The results for two of them are shown in Fig. 4. The original maps of dust emission were obtained at four wavelengths with the instruments PACS and SPIRE: 160, 250, 350, and 500 μm (see Schneider et al. 2010, 2012, for details) and convolved to a common angular resolution of 36 arcsec.

The PLT parameters of the *first* slope are consistent with the results from other numerical studies. On the other hand, *N*-pdfs derived from observations of regions with star-forming activity display pronounced PLTs of slopes $-2 \geq n \geq -4$ (Schneider et al. 2013, 2015a; Pokhrel et al. 2016), also in agreement with our results on the PLT evolution from the HRIGT runs.

The slope n of the *N*-pdf should be related to q as:

$$n = 2q/(3+q) \ ,$$

assuming that that the general cloud structure can be described through a power-law density profile (see Donkov, Veltchev and Klessen 2017, and the references therein). Plugging $q \sim -1.5$ (Girichidis et al. 2014) typical for advanced evolutionary stages in the formula above we get slopes n_2 of the *second* PLT in general agreement with the extracted ones from *Herschel* maps (Figs. 5 and 6). We conclude that the adapted BPLFIT method extracts PLTs of the ρ-pdfs and *N*-pdfs with slopes which are mutually consistent.

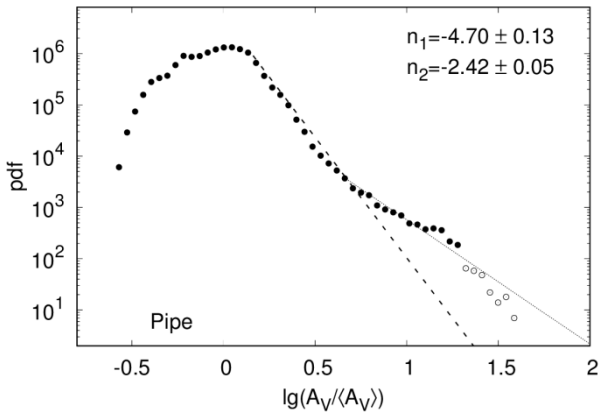

Figure 5: *N*-pdf with two PLTs from a *Herschel* map of the low-mass Galactic star-forming region Pipe. Open circles denote bins which were excluded from consideration due to the poor statistics.

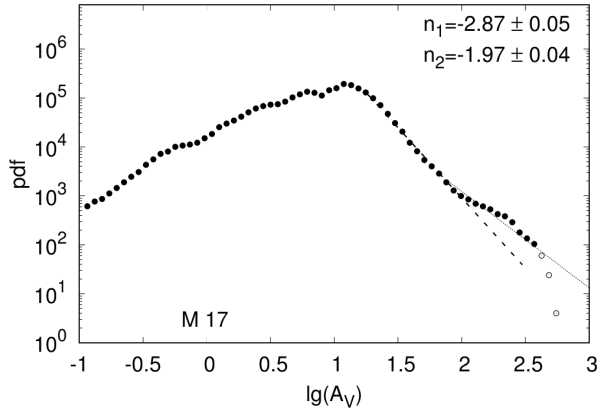

Figure 6: The same like Fig. 5 but for the high-mass Galactic star-forming region M17.

6. CONCLUSIONS

We present a novel approach for extraction of second power-law tails (PLTs) of the density (ρ-pdf) or column-density distribution (N-pdf) in star-forming clouds. The method is an extension of the adapted BPLFIT technique and was tested on data from numerical simulations of star-forming clouds at clump scale (0.5 pc; self-gravitating isothermal medium) and on observational data from *Herschel*. Our conclusions are as follows:

- The adapted BPLFIT method can be successfully extended to detect a second PLT.
- The test of this approach on numerical data with high resolution (HRIGT) yields PLT parameters in agreement with theoretical and numerical studies (Girichidis et al. 2014, Kritsuk, Norman and Wagner 2011).
- The application of the method on N-pdfs from *Herschel* data indicates the existence of a *second* PLT in N-pdfs in a dozen star-forming regions of different mass. (Schneider et al. 2020).
- A thorough comparison between the output of the methods from ρ-pdfs and N-pdfs from numerical data would shed light on the relationship between the slopes of the extracted PLTs.

Acknowledgements

The authors thank P. Girichidis for providing data from his HRIGT simulations and N. Schneider for the *Herschel* maps of the star-forming regions Pipe and M17.

L. Marinkova thanks to the Bulgarian National Science Fund for providing support through Grant KP-06-PM-38/6 (Fundamental research by young scientists and postdocs 2019). T. Veltchev acknowledges funding from the Ministry of Education and Science of the Republic of Bulgaria, National RI Roadmap Project DO1-277/16.12.2019.

References

Ballesteros-Paredes J., Andre P., Hennebelle P., Klessen R. S., Kruijssen J. M. D., Chevance M., Nakamura F., Adamo A., Vazquez-Semadeni E.: 2020, *Space Science Reviews,* 216, 5, 76.

Ballesteros-Paredes J., Vázquez-Semadeni E., Gazol A., Hartmann L., Heitsch F., Colin P.: 2011, *Monthly Notices of the Royal Astronomical Society*, 416, 1436.

Donkov S.,Veltchev T., Klessen R.S.: 2017, *Monthly Notices of the Royal Astronomical Society,* 466, 914.

Federrath C., Klessen R. S.: 2013, *The Astrophysical Journal*, 763, 51

Federrath C., Klessen R.S., Schmidt W.: 2008, *The Astrophysical Journal*, 688, L79.

Federrath C., Roman-Duval J., Klessen R. S., Schmidt W., Mac Low M.: 2010, *Astronomy & Astrophysics*, 512, A81.

Girichidis P., Konstandin L., Whitworth A. P., Klessen R. S., 2014: *The Astrophysical Journal* , 781, 91.

Girichidis P., Seifried D., Naab T., Peters T., Walch S., Wuensch R., Glover S. C. O., Klessen R. S.: 2018, *Monthly Notices of the Royal Astronomical Society*, 480, 3511.

Klessen R. S.: 2000, *The Astrophysical Journal*, 535, 869.

Koertgen B., Federrath C., Banerjee R.: 2019, *Monthly Notices of the Royal Astronomical Society*, 482, 5233.

Kritsuk A., Norman M., Wagner R.: 2011, *The Astrophysical Journal*, 727, L20.

Li Y., Klessen R., Mac Low M.-M.: 2003, *The Astrophysical Journal*, 592, 975.

Pokhrel R., Gutermuth R., Ali B., Megeath T., et al.: 2016, *Monthly Notices of the Royal Astronomical Society,* 461, 22.

Schneider N., Motte F., Bontemps S., Hennemann M., et al.: 2010, *Astronomy and Astrophysics,* 518, L83.

Schneider N., Csengeri T., Hennemann M., Motte F., et al.: 2012, *Astronomy & Astrophysics*, 540, L11.

Schneider N., Andre Ph., Konyves V., Bontemps S., et al.: 2013, *The Astrophysical Journal,* 766*,* L17.

Schneider N., Bontemps S., Girichidis P., Rayner T., et al.: 2015, *Monthly Notices of the Royal Astronomical Society,* 453, L41.

Schneider N., Ossenkopf-Okada V., Klessen R.S., Veltchev T., et al.: 2020, *Astronomy & Astrophysics* (submitted).

Vázquez-Semadeni E.: 1994, *The Astrophysical Journal*, 423, 681.

Veltchev T. V., Girichidis P., Donkov S., Schneider N., Stanchev O., Marinkova L., Seifried D., Klessen R. S.: 2019, *Monthly Notices of the Royal Astronomical Society*, 489, 788-801.